Heat Transfer Analysis of MgB_2 Coil in Heat Treatment Process for Future Fusion Reactor

Weijun Wang, Yongsheng Wu, Yuxiang He, Peng Gao, Arend Nijhuis, and Jinggang Qin

***Abstract*—State of the art MgB_2 is reviewed as a potential material for the poloidal field (PF) coils of the future fusion reactor due to its high critical temperature and low material cost. The heat treatment process is a crucial step in the development of MgB_2 magnets. The temperature lag in heat treatment of large magnets can lead to insufficient thermal reaction time. It may be infeasible to control the temperature of a magnet according to the heat treatment scheme recommended for the MgB_2 wire. Hence, the heat treatment process of a large magnet needs to be evaluated. Therefore, the dynamic temperature distribution of a MgB_2 PF coil is obtained by simulating the heat transfer in heat treatment process. A suitable heat treatment schedule for a large magnet is proposed and the experimental results of a sub-size Cable-In-Conduit Conductor manufactured with MgB_2 strand confirmed the feasibility of the newly proposed heat treatment process. The results provide a reference for the heat treatment method of a future larger MgB_2 coil.**

***Index Terms*—Fusion, PF coil, cable-in-conduit conductor (CICC), heat treatment, MgB_2.**

I. Introduction

SINCE THE superconductivity of MgB_2 was discovered by Nagamatsu et al. in 2001 [1], the material has been studied extensively. Many advantages of MgB_2 were found, such as low material cost, light weight, small anisotropy and an attractive high critical temperature ($Tc = 39$ K) [2]. Up to now, most of the MgB_2 applications are limited to generate magnetic fields up to 5 T at an operating temperature of 10 to 25 K [3], [4]. The transition temperature of the MgB_2 is much higher than those of conventional metallic superconductors such as Nb_3Sn and NbTi, and it has no reducing superconducting current by grain boundaries. Therefore, this relatively new superconductor is a potential candidate for use in low field fusion reactor magnets, such as poloidal field (PF) coils, correction coils and their feeders [5]. Especially when further increase of the MgB_2 strand performance could be anticipated.

TABLE I
THE PARAMETERS OF CFETR PF COILS

Coils	R(m)	Z(m)	ΔR(m)	ΔZ(m)	Turns
PF1	4.60	9.83	1.036	1.512	468
PF2	13.03	6.653	0.697	1.167	240
PF3	15.30	3.30	0.697	1.167	240
PF4	15.30	-3.30	0.697	1.167	240
PF5	14.91	-6.25	0.697	1.167	240
PF6	7.13	-10.00	0.697	1.167	240
PF7	4.60	-9.83	1.036	1.512	468

R(m) and Z(m) is the centre of the coil section, ΔR(m) and ΔZ(m) is the size of the coil section

The China Fusion Engineering Test Reactor (CFETR) based on ITER technology will be built to bridge the gap between ITER and the fusion demonstration reactor to develop the fusion technology in China [6]. According to the design requirement, the CFETR magnet system comprises seven ITER-like PF coils operating with maximum currents of 43 kA at 4.2 K. The main parameters [7] of the PF magnets are listed in Table I. The electromagnetic analysis reveals that the maximum fields in PF7 and PF1 are 7.5 T and 6.4 T, while those in other PF coils are less than 5 T. Therefore, PF2 to PF6 have potential to be wound with MgB_2 cable-in-conduit conductor (CICC). The largest size of PF3/PF4 leads to the worst temperature lag. Hence, the heat treatment process of PF3/PF4 wound with MgB_2 CICC is mainly studied here. It is worth mentioning that three types of MgB_2 CICC sub-size cables are developed at the Institute of Plasma Physics Chinese Academy of Sciences (ASIPP) to verify the feasibility of MgB_2 wires in PF coils for fusion magnets [8].

The MgB_2 wires used for making the cabled conductors are manufactured by Western Superconducting Technologies Co., Ltd. (WST). The main parameters of the MgB_2 wires are listed in Table II. In the recommended heat treatment schedule for WST wire used here, first, the MgB_2 wire is heated to 600 °C at 600 °C/h, then kept constant at 600 °C for 2 h to react, and naturally cooled to room temperature in argon atmosphere. The technical requirement is that the heat treatment temperature uniformity for the plateau stage is within ±5 °C.

The irreversible strain limits for a MgB_2 wire are reported to be −0.75% in compression and +0.3% in tension [9]. During the

Manuscript received 3 November 2022; revised 28 December 2022, 30 January 2023, and 4 February 2023; accepted 6 February 2023. Date of publication 10 February 2023; date of current version 16 February 2023. This work was supported in part by the National Key Research and Development Plan under Grant 2019YFC0117502, in part by the Youth Innovation Promotion Association, Chinese Academy of Sciences under Grant 2013211, in part by HFIPS Director's Fund under Grant No. YZJJ2023QN15, and in part by the National High Level Research Project. *(Corresponding author: Yongsheng Wu.)*

Weijun Wang, Yongsheng Wu, Peng Gao, and Jinggang Qin are with the Institute of Plasma Physics, Chinese Academy of Sciences, Hefei 230031, China (e-mail: yswu@ipp.ac.cn).

Yuxiang He is with the Hefei Institutes of Physical Science, Chinese Academy of Sciences, Hefei 230031, China, and also with the Science Island Branch, Graduate School of University of Science and Technology of China, Hefei 230026, China.

Arend Nijhuis is with the Faculty of Science and Technology, University of Twente, 7500AE Enschede, The Netherlands.

Color versions of one or more figures in this article are available at https://doi.org/10.1109/TASC.2023.3244150.

Digital Object Identifier 10.1109/TASC.2023.3244150

TABLE II
THE PARAMETERS OF MgB_2 WIRES

Wire type	5MB2000 (WST)
Diameter [mm]	0.84
Filaments in center	Nb×7
Number of SC filaments	30
Barrier	Nb
Matrix	Cu
Sheath	Monel
Proportion of MgB_2 [%]	15
Filament diameter [μm]	53
Twist pitch [mm]	No twist

manufacturing process of the CICC coil, the MgB_2 wire needs to be twisted, squeezed, and bent. If the technical route of reaction before winding is adopted, the wires are prone to degradation or even fracture during the preparation of the CICC coil [8]. Therefore, the large MgB_2 magnet must be wound before heat treatment (Wind and React) to avoid manufacturing risks. Unlike wire, a magnet coil wound with MgB_2 CICC has a significantly larger mass. The recommended heat treatment scheme of MgB_2 wires has a fast heating rate and short holding time. Therefore, the reaction time of the given heat treatment schedule for MgB_2 wires is probably too short for larger conductors and magnets. Ideally, a longer reaction time will allow all the MgB_2 wires in the conductor and magnet to react sufficiently and to meet the heat treatment temperature requirements [10]. However, the critical current appears to decrease with the increase of the reaction time [11]. Hence the appropriate reaction time of MgB_2 magnet needs to be explored.

In this work, the heat treatment of a MgB_2 PF coil is simulated to verify a suitable heat treatment schedule. The maximum temperature differences inside the coil are obtained from the temperature distribution during the heat treatment process. A customized heat treatment schedule of MgB_2 PF coil is proposed and evaluated. Relevant heat treatment experiments have been performed on single strands and a MgB_2 sub-size Cable-In-Conduit Conductor has been fabricated and successfully tested.

II. SIMULATION OF HEAT TREATMENT

A. Heat Treatment Process

The heat treatment of the MgB_2 coil includes heating and cooling process. The heating process consists of a heating stage and a soaking stage. The cooling process, it is mainly natural cooling with the furnace. The heating process is the key to achieve the performance of the MgB_2 coil, so the heat transfer analysis of the heating process is mainly analyzed here. In order to make the heat transfer faster and the temperature of the coil more uniform, the atmospheric heat treatment method is used. First the side wall of the furnace is heated, and then the MgB_2 coil is heated by forced convection of argon gas in the furnace. Fig. 1 shows the schematic diagram of argon gas flowing in the furnace. Similar equipment and method have been successfully used in the heat treatment of Nb_3Sn coils [12]. Heat transfer in the heat treatment furnace mainly includes: (1) the heat radiation between the furnace and the coil; (2) forced convection heat transfer between the furnace and the coil under the action of the fan; (3) the heat conduction inside the coil.

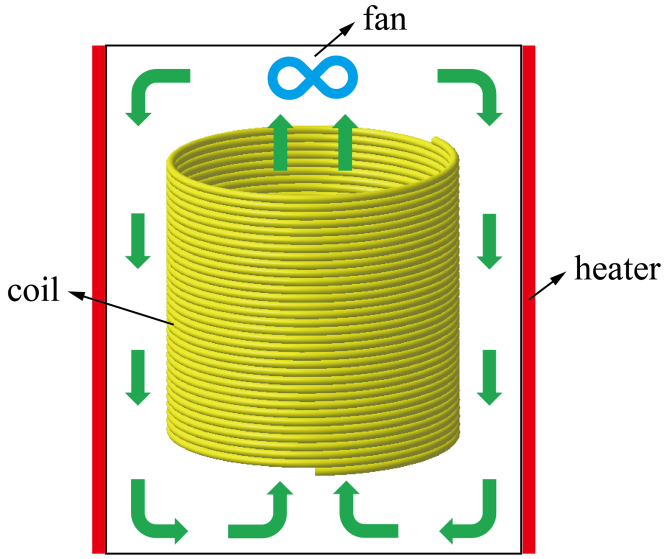

Fig. 1. Schematic diagram of coil heated by forced convection of argon gas.

The two-dimensional heat conduction equation within the coil can be written as follows:

$$(\rho C_p)\ \frac{\partial T}{\partial t} = \frac{1}{r}\frac{\partial}{\partial r}\left(r\lambda_r \frac{\partial T}{\partial r}\right) + \frac{\partial}{\partial z}\left(\lambda_z \frac{\partial T}{\partial z}\right) \quad (1)$$

Where the coil's properties are defined as density ρ, specific heat C_p, temperature T, time t, radial direction r, equivalent radial thermal conductivity λ_r, and equivalent axial thermal conductivity λ_z.

With the initial condition (t = 0):

$$T\ (r, z) = T_0 \quad (2)$$

Where T_o is the initial temperature of the coil.

And the boundary conditions (t>0):

$$-\lambda \left(\frac{\partial T}{\partial n}\right)_c = h\,(T_c - T_{Ar}) + q_r \quad (3)$$

Where $(\partial T/\partial n)_c$ is temperature changing rate in normal direction of the coil surface, h is the convective heat transfer coefficient, T_c is the surface temperature of the coil, T_{Ar} is the temperature of argon, q_r is the net radiant heat flux between the coil surface and the surrounding environment.

Argon is a monatomic molecule, and its gas radiation is not considered. Therefore, the radiant heat flux q_r in (3) is calculated as follows:

$$q_r = \sigma\left(\varepsilon_e T_e^4 - \varepsilon_c T_c^4\right) \quad (4)$$

Where σ is the Stefan-Boltzman constant, ε_e is the emissivity of surrounding environment, T_e is the average temperature of surrounding environment, ε_c is the emissivity of coil, T_c is the temperature of the coil surface.

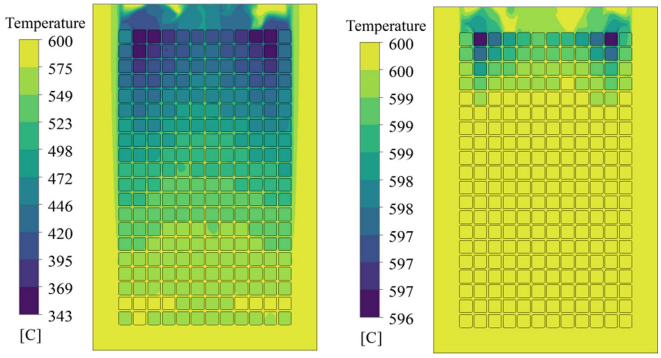

Fig. 2. Temperature distribution of the coil at the end of the heating stage (left) and at a soaking stage time of 120 minutes (right).

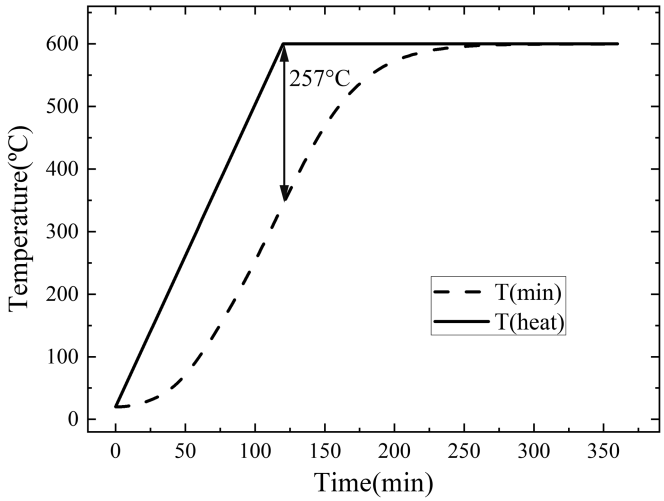

Fig. 3. Minimum temperature of the coil as a function of the heat treatment time is compared with the heat treatment curve.

B. Analysis of Heat Treatment

The temperature gradient of the MgB_2 coil during the heat treatment process is simulated by the finite element method. Due to the complicated structure of the heat treatment furnace, a simplified model is built. From the gas circulation loop, it can be seen that the argon gas flows from the bottom of the coil to the top. The argon gas flow rate is constant, and the temperature of the gas rises as the furnace heats up. Therefore, only the coil structure and surrounding gas will be considered in order to avoid the establishment of a complex furnace model. Here we assume that the temperature variation of the gas at the bottom inlet is consistent with the heat treatment curve. Considering the temperature difference between the furnace and the surface of coil, the radiation heat transfer needs to be taken into account in this simulation. Considering the symmetry in geometric structure, we only build the vertical cross section model of the coil.

In order to solve the heat transfer problem between argon gas and coil, the finite volume method and the realizable k-epsilon turbulence model with enhanced wall function are adopted. The transient analysis method is used to apply the temperature varying with time to the gas inlet through user-defined functions. The initial temperature of the whole model is set at 20 °C. As the temperature changes rapidly at the beginning of heating, a time step of 1 s is adopted at the initial stage. After the calculation becomes stable, the time step is increased to 10 s to complete the remaining calculation.

The PF3/PF4 coil of the CFETR has 240 turns, involving 12 turns in radial direction and 20 turns in vertical direction. If the recommended heat treatment curve of MgB_2 wires is applied to such a large magnet, the thermal reaction process inside the magnet will be insufficient. Therefore, it is essential to reduce the heating rate and extend the holding time. Through a series of analysis, the heat treatment schedule of MgB_2 PF magnet is preliminarily determined as follows: first, the MgB_2 PF magnet is heated from room temperature to 600 °C at a rate of 300 °C/h, then kept constant at 600 °C for 4 h, and naturally cooled to room temperature. The temperature field distribution of the MgB_2 coil at the end of the heating stage is shown in Fig. 2. The maximum temperature difference in the coil is 257 °C at the end of the heating stage. The temperature hysteresis of the coil is obvious due to its large heat capacity. The argon gas enters the magnet from the bottom through the inter-turn gaps of the magnet and transfers heat to the magnet, which causes the temperature of the gas itself to decrease continuously inside the magnet. It weakens the ability of the gas to heat the top of the magnet resulting in a temperature difference of the magnet during the heat treatment process.

In order to allow the magnet to have sufficient reaction time, it is necessary to extend the holding time to 4 hours. The minimum temperature curve of the coil changing with heat treatment time is shown in Fig. 3. It is found that the temperature difference of the coil gradually shrinks during the soaking stage. As shown in the Fig. 2, the temperature uniformity of the MgB_2 coil is within ±5 °C at a soaking stage time of 2 hours. It can be considered that the whole coil is in thermal reaction process. When the bottom of the coil is in the plateau period for 2 hours, the top of the coil just enters the holding stage. If the holding time is set to 4 hours, the top of the coil is held at 600 °C for about 2 h as required. Meanwhile, the bottom of the coil is kept at 600 °C for about 4 h. Previous works [11] show that when the dwelling time in the heat treatment schedule is increased to twice the recommended value (2 h), the *Ic* of the wires decreases by less than 5%. Therefore, setting the dwell time to 4 h is acceptable.

III. Small Conductor Experiment

A. Parameter of the Conductor

In order to verify the strand properties, cabling, conductor compaction and heat treatment processes of MgB_2 CICC, a sub-size CICC based on WST MgB_2 wire has been manufactured. The outer diameter of the MgB_2 CICC is 15.5 mm, and the cable diameter is 12.45 mm. The structure of the cable is (2SC+1Cu)×3×4×4 with a void ratio of 28.3%, including 96 MgB_2 wires with a diameter of 0.84 mm and 48 copper wires with a diameter of 0.82 mm. The length of sub-size CICC sample

Fig. 4. The cross section of the MgB_2 CICC.

TABLE III
KEY PARAMETERS OF THE MgB_2 CICC SUB-SIZE CABLE

Parameters	Values
MgB_2 wire diameter [mm]	0.84
Cu wire diameter [mm]	0.82
Number of MgB_2 strands	96
Number of Cu strands	48
Cable layout	(2SC + 1Cu) ×3 × 4 × 4
Twist pitch sequence [mm]	50/58/66/76
Void fraction [%]	28.3
Cable diameter [mm]	12.45
Conductor diameter [mm]	15.5
Length of the cable [mm]	1200

is 1.2 m. The cross section of CICC is shown in Fig. 4. Table III is the key parameters of the MgB_2 CICC sub-size cable.

B. Heat Treatment Equipment

The heat treatment of the MgB_2 CICC conductor samples has been carried out on a ZRMT-210-9W4 tubular vacuum heat treatment furnace, as shown in Fig. 5. The diameter of the furnace tube is 300 mm, the effective uniform temperature zone is 4 m, the uniformity of the temperature in the furnace is ±5 °C, and the vacuum level in the furnace can be maintained below 5×10^{-4} Pa.

C. Heat Treatment Process

The MgB_2 CICC conductor sample is first secured on the sample holder of the heat treatment furnace. The thermocouples are fixed at the front, middle and back of the conductor sample to monitor the actual local heat treatment temperature. In addition,

Fig. 5. The large tubular vacuum heat treatment furnace.

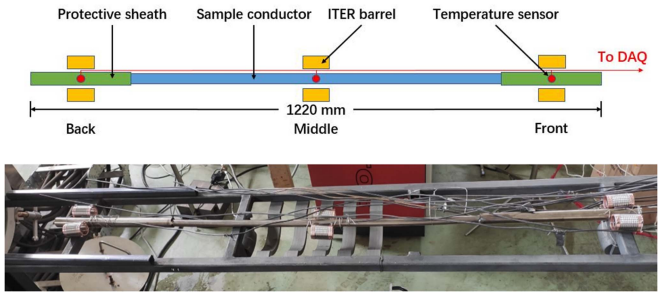

Fig. 6. Schematic diagram (up) and picture (down) of the preparation for the heat treatment of the MgB_2 conductor.

TABLE IV
CRITICAL CURRENT PERFORMANCE OF WITNESS SAMPLES AND STANDARD HEAT TREATED SAMPLES ARE COMPARED IN HEAT TREATMENT EXPERIMENT

type	Witness samples (5MB2000 WST)			standard samples
location	front	middle	back	
2 T	407.0A	393.8A	400.1A	372.3A
3 T	238.7A	229.7A	228.6A	217.4A
4 T	143.8A	140.2A	139.4A	131.7A
5 T	87.1A	85.0A	84.2A	81.3A
6 T	50.7A	49.9A	49.6A	48.3A

ITER barrels samples [13] are arranged near each thermocouple as witness samples. The MgB_2 wire used in the witness sample is the same as used for the CICC. The relative positions of conductor sample, thermocouple and witness sample are shown in Fig. 6.

The conductor is heat treated according to the proposed heat treatment curve of the PF magnet, heated from room temperature to 600 °C at 300 °C/h, held at 600 °C for 4 h, and then cooled in the furnace to room temperature. The actual heating curve of the heat treatment is shown in Fig. 7.

After the heat treatment of the MgB_2 conductor, the critical current performance of the witness samples under different background fields is tested, and the test results are shown in Table IV. The critical current recommended by WST at 4.2 K is 81.3 A@5 T. The critical currents for all witness samples

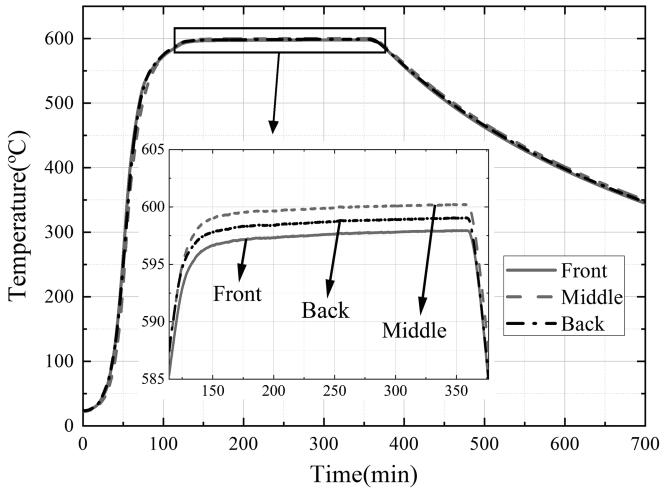

Fig. 7. Actual measured heating curve of the CICC heat treatment.

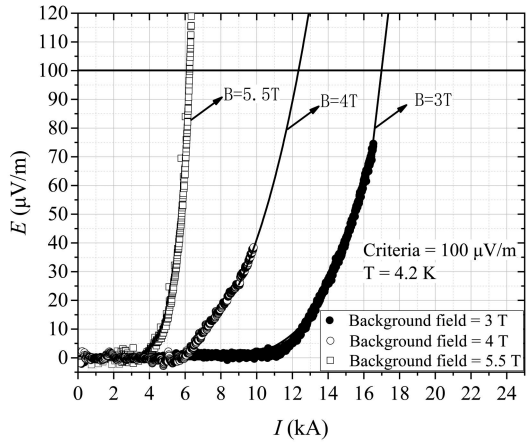

Fig. 8. Typical *V–I* curve of MgB_2 CICC in applied magnetic field.

range from 84 A to 87 A, and the n-value is 23 to 27. Compared with the standard sample, the performance of the witness sample fluctuates within a reasonable range.

The critical current of the MgB_2 CICC sample is tested on the 30 kA conductor DC test platform of ASIPP [14]. The typical *V-I* curves of MgB_2 CICC sample in this experiment are shown in Fig. 8. By adding the estimated self-fields, the critical current of conductor reaches 17.1 kA at 3.4 T peak magnetic field and 6.3 kA at 5.7 T peak magnetic field. The critical current of the CICC sample did not decline compared with the wire witness sample in the conductor heat treatment.

In ref. [8], the critical current at 4.2 K of the sub-size MgB_2 CICC cable shows significant degradation compared to the witness wires. We optimized the wire size and cabling process of the sub-size MgB_2 CICC here, significantly improving conductor performance. The diameter of MgB_2 wire here is 0.84 mm, while it is 1mm in ref. [8]. The thinner wire can make contact between wires more uniform and prevent stress concentration. Meanwhile, the twist pitch sequence of MgB_2 CICC here is 50/58/66/76 mm while it is 51/60/69/79 mm in ref. [8]. The high rigidity of the short twist pitch cable could prevent these plastic deformations caused by the Lorentz force [15]. Thus, short twist pitch design might be a potential solution for MgB_2 conductors. The performance of conductors with different wire diameters and different twist pitches needs to be further studied in detail.

IV. Conclusion

In this study, the heat treatment process of a MgB_2 PF coil is simulated. Because of its large heat capacity, the response of the MgB_2 coil to temperature increase is delayed significantly during the heat treatment. The proposed heat treatment scheme of a MgB_2 PF coil is therefore set as follows: the magnet is heated from room temperature to 600 °C at 300 °C/h, held at 600 °C for 4 h, and then cooled to room temperature. This scheme increases the reaction time to overcome the temperature lag in heat treatment process. A sub-size MgB_2 CICC has been manufactured and heat treated. The test shows that the critical current density performance of the conductor does not decline with electromagnetic load cycling. This demonstrates that the heat treatment schedule is suitable. The results provide a reference for a practical heat treatment method of future larger MgB_2 coils.

References

[1] J. Nagamatsu et al., "Superconductivity at 39 K in magnesium diboride," *Nature*, vol. 410, no. 6824, pp. 63–64, 2001.
[2] A. Gurevich et al., "Very high upper critical fields in MgB_2 produced by selective tuning of impurity scattering," *Supercond. Sci. Technol.*, vol. 17, no. 2, pp. 278–286, 2004.
[3] A. Ballarino and R. Flükiger, "Status of MgB_2 wire and cable applications in Europe," *J. Phys.: Conf. Ser.*, vol. 871, 2017, Art. no. 012098.
[4] Z. Zhang et al., "Review of synthesis of high volumetric density, low gravimetric density MgB_2 bulk for potential magnetic field applications," *Superconductivity*, vol. 3, 2022, Art. no. 100015.
[5] N. Bairagi, V. L. Tanna, and D. Raju, "Preliminary design and analysis of 20 K helium cooled MgB_2 based superconducting current feeder system for tokamak application," *IEEE Trans. Appl. Supercond.*, vol. 32, no. 6, Sep. 2022, Art. no. 4802305.
[6] G. Zhuang et al., "Progress of the CFETR design," *Nucl. Fusion*, vol. 59, 2019, Art. no. 112010.
[7] Y. T. Song et al., "Engineering design of the CFETR machine," *Fusion Eng. Des.*, vol. 183, 2022, Art. no. 113247.
[8] P. Gao et al., "DC performance and AC loss of sub-size MgB_2 CICC conductor for fusion magnet application," *Nucl. Fusion*, vol. 62, 2022, Art. no. 056014.
[9] C. Zhou et al., "Intrawire resistance, AC loss and strain dependence of critical current in MgB_2 wires with and without cold high-pressure densification," *Supercond. Sci. Technol.*, vol. 27, 2014, Art. no. 075002.
[10] H. Müller and T. Schneider, "Heat treatment of Nb_3Sn conductors," *Cryogenics*, vol. 48, no. 7-8, pp. 323–330, 2008.
[11] Y. He, W. Wang, A. Nijhuis, J. Qin, and C. Zhou, "Effect of heat treatment reaction time on the performance of MgB_2 wires," *IEEE Trans. Appl. Supercond.*, vol. 32, no. 1, Jan. 2022, Art. no. 6200105.
[12] W. J. Wang et al., "Heat transfer analysis during heat treatment of Nb_3Sn coils for the CFETR CSMC," *Fusion Eng. Des.*, vol. 165, 2021, Art. no. 112248.
[13] A. Nijhuis, W. A. J. Wessel, H. G. Knoopers, Y. Ilyin, A. della Corte, and H. H. J. Kate, "Compressive pre-strain in Nb_3Sn strand by steel tube and effect on the critical current measured on standard ITER barrel," *IEEE Trans. Appl. Supercond.*, vol. 15, no. 2, pp. 3466–3469, Jun. 2005.
[14] H.-J. Ma et al., "Test facility for critical current measurement of superconducting conductors," *IEEE Trans. Appl. Supercond.*, vol. 29, no. 5, Aug. 2019, Art. no. 4800705.
[15] Y. Nabara et al., "Impact of cable twist pitch on tcs-degradation and AC loss in Nb_3Sn conductors for ITER central solenoids," *IEEE Trans. Appl. Supercond.*, vol. 24, no. 3, Jun. 2014, Art. no. 4200705.